J Mater Sci: Mater Electron (2010) 21:649–655
DOI 10.1007/s10854-009-9971-7

Dielectric and piezoelectric properties of MnO_2-doped $K_{0.5}Na_{0.5}Nb_{0.92}Sb_{0.08}O_3$ lead-free ceramics

Dunmin Lin · Qiaoji Zheng · K. W. Kwok · Chenggang Xu · Chun Yang

Received: 17 May 2009 / Accepted: 24 August 2009 / Published online: 9 September 2009

Abstract Lead-free MnO_2-doped $K_{0.5}Na_{0.5}Nb_{0.92}Sb_{0.08}O_3$ ceramics have been fabricated by a conventional ceramic technique and their dielectric and piezoelectric properties have been studied. Our results show that a small amount of MnO_2 (0.5–1.0 mol%) is enough to improve the densification of the ceramics and decrease the sintering temperature of the ceramics. The co-effects of MnO_2 doping and Sb-substitution lead to significant improvements in the ferroelectric and piezoelectric properties. The $K_{0.5}Na_{0.5}Nb_{0.92}Sb_{0.08}O_3$ ceramic with 0.5 mol%MnO_2 doping possesses optimum propeties: $d_{33} = 187$ pC/N, $k_P = 47.2\%$, $\varepsilon_r = 980$, $\tan\delta = 2.71\%$ and $T_c = 287$ °C. Due to high tetragonal-orthorhombic phase transition temperature ($T_{O\text{-}T} \sim 150$ °C), the $K_{0.5}Na_{0.5}Nb_{0.92}Sb_{0.08}O_3$ ceramic with 0.5 mol%MnO_2 doping exhibits a good thermal stability of piezoelectric properties.

1 Introduction

Lead-containing piezoelectric materials with perovskite structure, such as $Pb(Zr,Ti)O_3$ and $Pb(Mg_{1/3}Nb_{2/3})$-$PbTiO_3$, have been widely used in electronic and microelectronic devices because of their excellent piezoelectric and ferroelectric properties. However, the strong toxicity and high evaporation of lead oxide during sintering have caused a crucial environmental pollution. Therefore, it is necessary to develop lead-free piezoelectric ceramics with good piezoelectric properties for replacing the lead-containing ceramics in various applications.

Alkali niobate $K_{0.5}Na_{0.5}NbO_3$ (KNN), a solid solution of ferroelectric $KNbO_3$ and antiferroelectric $NaNbO_3$, is considered as a promising candidate for lead-free piezoelectric ceramics because of its high Curie temperature (about 420 °C), good ferroelectric properties ($P_r = 33$ μC/cm^2) and large electromechanical coupling factors [1, 2]. However, it is very difficult to obtain dense and well-sintered KNN ceramics using an ordinary sintering process because of the volatility of alkaline elements at high temperature. For a well-sintered KNN ceramic (e.g. prepared by hot-pressing technique), it possesses good piezoelectric properties ($d_{33} = 160$ pC/N, $k_p = 45\%$) and high density ($\rho = 4.46$ g/cm^3). [2] However, there is severe degradation in piezoelectric properties ($d_{33} = 80$ pC/N, $k_p = 36\%$) and density ($\rho = 4.25$ g/cm^3) for an air-fired KNN ceramics. [1, 3] A number of studies have been carried out to improve the sinterability and electrical properties of KNN ceramics, including the formation of solid solutions such as Li- and Ta-modified KNN [4], KNN-$LiSbO_3$ [5, 6], KNN-$BaTiO_3$ [7], $K_{0.475}Na_{0.475}Li_{0.05}NbO_3$-$Bi_{0.48}Na_{0.48}Ba_{0.04}TiO_3$ [8], KNN-$LiNbO_3$ [9], KNN-$Bi_{0.5}Na_{0.5}TiO_3$ [10] and KNN-Li(Nb,Ta,Sb)O_3 [11], and the use of sintering aids, e.g. $K_{5.4}Cu_{1.3}Ta_{10}O_{29}$ [12] and CuO [13]. It has been known that Sb has a much larger Pauling electronegativity than Nb (2.05 vs. 1.5). Therefore, the partial substitution of Sb^{5+} for Nb^{5+} induces a strong covalency in the KNN perovskite, which favors the ferroelectricity and piezoelectricity. [11, 14] It is also noted that MnO_2 is an effective dopant in the Pb-containing piezoelectric ceramics to enhance densification and reduce loss tangent $\tan\delta$. [15, 16] In the present work, MnO_2-doped

D. Lin (✉) · Q. Zheng · C. Xu · C. Yang
College of Chemistry and Materials Science, and Visual Computing and Virtual Reality Key Laboratory of Sichuan Province, Sichuan Normal University, 610066 Chengdu, People's Republic of China
e-mail: ddmd222@yahoo.com.cn

K. W. Kwok
Department of Applied Physics and Materials Research Centre, The Hong Kong Polytechnic University, Kowloon, Hong Kong, China

$K_{0.5}Na_{0.5}Nb_{0.92}Sb_{0.08}O_3$ ceramics, $K_{0.5}Na_{0.5}Nb_{0.92}Sb_{0.08}O_3$ + xmol%MnO_2, were prepared by ordinary solid-state sintering, and the effects of MnO_2 doping on the microstructures, dielectric and piezoelectric properties of $K_{0.5}Na_{0.5}Nb_{0.92}Sb_{0.08}O_3$ ceramics were investigated.

2 Experimental

$K_{0.5}Na_{0.5}Nb_{0.92}Sb_{0.08}O_3$ + xmol%MnO_2 ceramics ($0 \leq x \leq 3.0$) were prepared by an ordinary sintering technique using analytical-grade metal oxides or carbonate powders: Na_2CO_3 (99.8%), K_2CO_3 (99.9%), Nb_2O_5 (99.5%), Sb_2O_3 (99%) and MnO_2 (99%). The stoichiometric $K_{0.5}Na_{0.5}Nb_{0.92}Sb_{0.08}O_3$ powder was first synthesized at 880 °C for 6 h by a solid state reaction. After the calcination, $K_{0.5}Na_{0.5}Nb_{0.92}Sb_{0.08}O_3$ and MnO_2 powders were weighed according to the formula of $K_{0.5}Na_{0.5}Nb_{0.92}Sb_{0.08}O_3$ + xmol%MnO_2 and then ball-milled for 8 h. The resulting powders were mixed thoroughly with a PVA binder solution and then pressed into disk samples with the diameter of 15.0 mm and thickness of 1.20 mm. The disk samples were finally sintered at 1,080–1,120 °C for 4 h in air. Silver electrodes were fired on the top and bottom surfaces of the sintered samples. The ceramics were poled under a dc field of 5–6 kV/mm at room temperature in a silicon oil bath for 30 min.

The crystalline structure of the sintered samples was examined using X-ray diffraction (XRD) analysis with CuK_α radiation (DX-1000). The bulk density ρ was measured by the Archimedes' method. The microstructures were observed using scanning electron microscopy (JEOL JSM-5900LV). The relative permittivity ε_r and loss tangent tanδ of the ceramics at 1, 10 and 100 kHz were measured as functions of temperature using an impedance analyzer (Agilent 4192A). A conventional Sawyer–Tower circuit was used to measure the polarization hysteresis (*P-E*) loop at 100 Hz. The electromechanical coupling factor k_p and electromechanical quality factor Q_m were determined by the resonance method according to the IEEE Standard using an impedance analyzer (Agilent 4294A). The piezoelectric coefficient d_{33} was measured using a piezo-d_{33} meter (ZJ-3A, China).

3 Results and discussions

Figure 1 shows the XRD patterns of $K_{0.5}Na_{0.5}Nb_{0.92}Sb_{0.08}O_3$ + xmol%MnO_2 ceramics. From Fig. 1, all the $K_{0.5}Na_{0.5}Nb_{0.92}Sb_{0.08}O_3$ + xmol%MnO_2 ceramics possess a pure perovskite structure with orthorhombic symmetry and no second phase can be detected. The XRD patterns of the ceramics have been indexed by JCPDF card 71-2171.

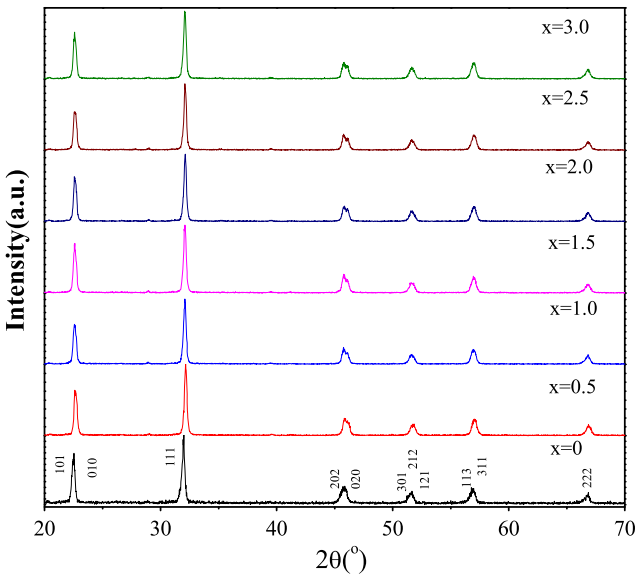

Fig. 1 XRD pattern of $K_{0.5}Na_{0.5}Nb_{0.92}Sb_{0.08}O_3$ + xmol%MnO_2 ceramics

The addition of MnO_2 to $K_{0.5}Na_{0.5}Nb_{0.92}Sb_{0.08}O_3$ does not cause any significant change to the crystalline structure.

The SEM micrographs of the $K_{0.5}Na_{0.5}Nb_{0.92}Sb_{0.08}O_3$ + xmol%MnO_2 ceramics with $x = 0$, 1.0, 2.0 and 3.0 are shown in Fig. 2, while Fig. 3 shows the variations of the bulk density ρ and optimum sintering temperature T_s with x. As shown in Fig. 2a, although the sintering temperature is high (1,120 °C), the $K_{0.5}Na_{0.5}Nb_{0.92}Sb_{0.08}O_3$ + xmol%MnO_2 ceramic with $x = 0$ (i.e., without MnO_2 doping) has a very loose structure and a large amount of pores can be found. For the $K_{0.5}Na_{0.5}Nb_{0.92}Sb_{0.08}O_3$ ceramic (i.e. $x = 0$), the grains have a diameter of about 1.2 μm. However,after the doping of a small amount of MnO_2 (≥0.5 mol%), the grain size increases significantly to about 2.5 μm, the ceramics can be well sintered at 1,080–1,110 °C and become considerably dense, and there is almost no pore on the surface of the ceramics (Fig. 2b–d). As shown in Fig. 3, the $K_{0.5}Na_{0.5}Nb_{0.92}Sb_{0.08}O_3$ ceramic without MnO_2-doping has a low bulk density of 4.12 g/cm^3. On the basis of the XRD results, the relatively density of the ceramic with $x = 0$ is about 90%. However, after the doping of 0.5–1.0 mol%MnO_2, the ceramics give a high density of 4.44–4.48 g/cm^3 (relative density > 97%). As x further increase to 3.0, the bulk density decreases slightly to 4.37 g/cm^3 (relative density ~ 95%). For each composition, the ceramics were sintered at different temperatures and their density was measured. The optimum sintering temperature was determined as the sintering temperature by which the ceramic has the largest density. From Fig. 3, as x increases, the optimum sintering temperature for the $K_{0.5}Na_{0.5}Nb_{0.92}Sb_{0.08}O_3$ + xmol%MnO_2 ceramics decreases. It can be clearly seen that the addition of a

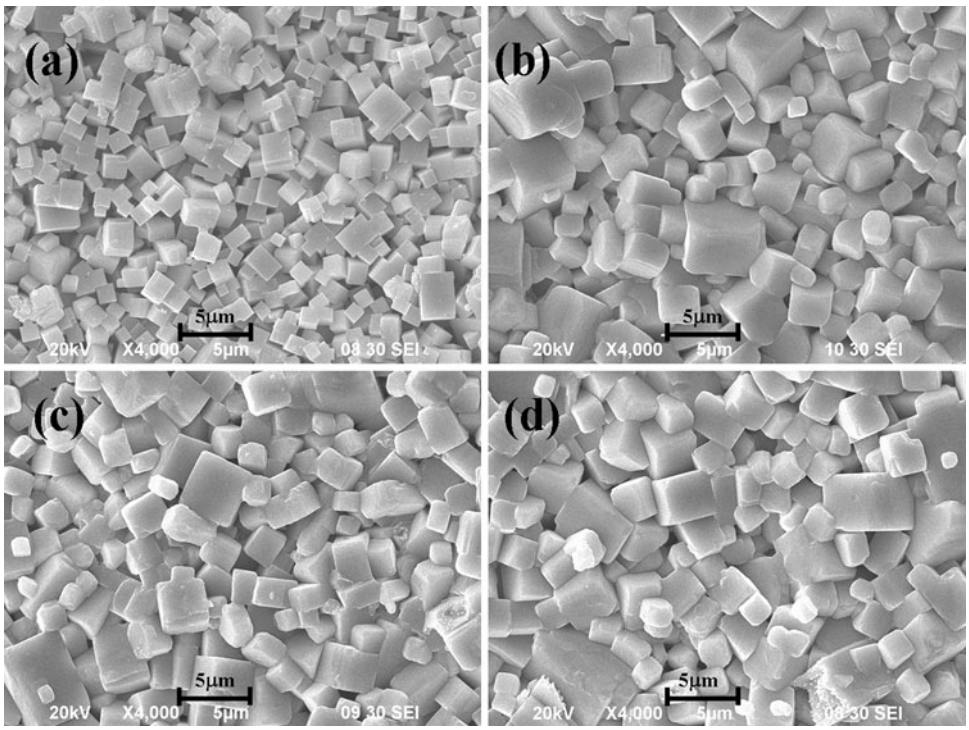

Fig. 2 SEM micrographs of the $K_{0.5}Na_{0.5}Nb_{0.92}Sb_{0.08}O_3$ + xmol%MnO_2 ceramics: **a** $x = 0$, sintered at 1,120 °C for 4 h; **b** $x = 1.00$, sintered at 1,110 °C for 4 h; **c** $x = 2.00$, sintered at 1,090 °C for 4 h; and **d** $x = 3.00$, sintered at 1,080 °C for 4 h

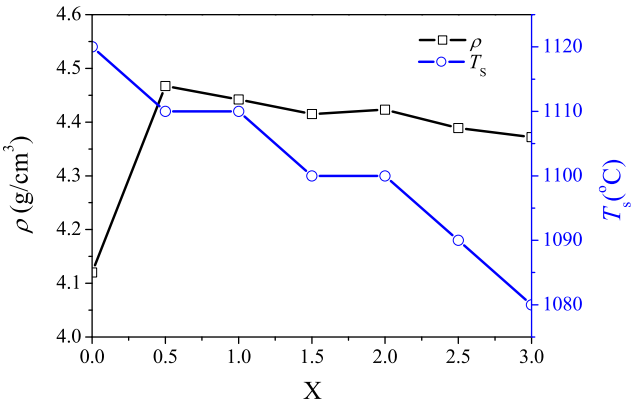

Fig. 3 Variations of the bulk density ρ and optimum sintering temperatures T_s with x for the $K_{0.5}Na_{0.5}Nb_{0.92}Sb_{0.08}O_3$ + xmol%MnO_2 ceramics

small amount of MnO_2 to the $K_{0.5}Na_{0.5}Nb_{0.92}Sb_{0.08}O_3$ ceramics results in the significant improvement in densification and a decrease in sintering temperature.

The temperature dependences of ε_r and tanδ for $K_{0.5}Na_{0.5}Nb_{0.92}Sb_{0.08}O_3$ + xmol%MnO_2 ceramics at 1 kHz are shown in Fig. 4. Similar to the pure KNN [1, 2], two transition peaks are observed: one is associated with the paraelectric cubic-ferroelectric tetragonal phase transition at T_c and the other is the ferroelectric tetragonal-ferroelectric orthorhombic phase transition at $T_{O\text{-}T}$. As shown in Fig. 4a, the observed $T_{O\text{-}T}$ for $K_{0.5}Na_{0.5}Nb_{0.92}Sb_{0.08}O_3$ + xmol% MnO_2 ceramics is insensitive to the doping level x of MnO_2. For the ceramics with $x = 0.5$–3.0, the observed $T_{O\text{-}T}$ is about 150 °C. Unlike $T_{O\text{-}T}$, the observed T_c increases from 287 to 298 °C with x increasing from 0.5 to 3.0. It can be also seen that as x increases, the value of the dielectric peak at T_c increases significantly. From Fig. 4b, for the ceramics with $x = 0.5$, 1.0, 2.0 and 3.0, the observed tanδ has a very weak dependence on temperature below T_c and retain almost unchangeable with temperature increasing. However, as temperature increases above T_c, a sharp increase in tanδ is observed in the ceramics with $x = 0.5$, 1.0, 2.0 and 3.0, which should be attributed to a decrease in electrical resistivity of the ceramics at higher temperatures, at which the ceramics become electrically conductive.

Figure 5 shows the temperature dependences of ε_r and tanδ for the $K_{0.5}Na_{0.5}NbO_3$ + 0.5 mol%MnO_2 and $K_{0.5}Na_{0.5}Nb_{0.92}Sb_{0.08}O_3$ + 0.5 mol%MnO_2 ceramics at 1, 10 and 100 kHz. It can be seen that the $K_{0.5}Na_{0.5}NbO_3$ + 0.5 mol%MnO_2 ceramic (i.e., Sb-free KNN ceramic with 0.5 mol%MnO_2 doping) retains the classic ferroelectric characteristic, and undergoes the cubic-tetragonal phase transition at 421 °C (T_c) and the tetragonal-orthorhombic phase transition at 210 °C ($T_{O\text{-}T}$) (Fig. 5a). After the substitution of 8% Sb^{5+} for Nb^{5+}, the ceramic (i.e., $K_{0.5}Na_{0.5}Nb_{0.92}Sb_{0.08}O_3$ + 0.5 mol%MnO_2) undergoes the same two phase transitions, with both T_c and $T_{O\text{-}T}$ shifted to lower temperatures (287 and 151 °C, respectively) (Fig. 5b).

The $K_{0.5}Na_{0.5}NbO_3$ + 0.5 mol%MnO_2 ceramic is a normal ferroelectric, thus exhibiting a sharp transition peak

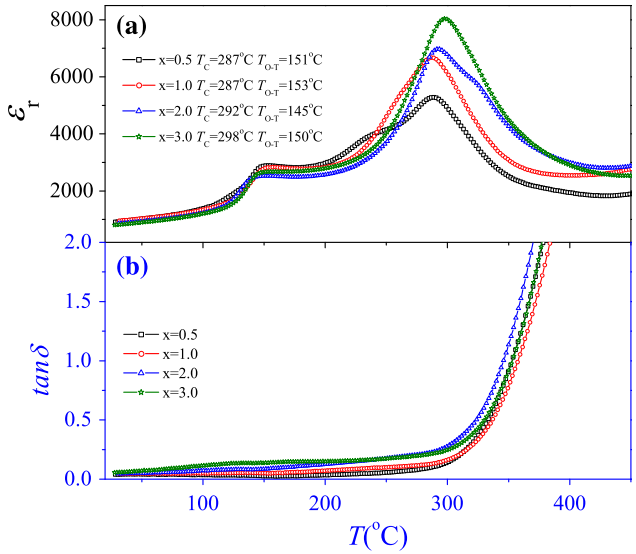

Fig. 4 Relative permittivity ε_r and loss tangent tanδ of the $K_{0.5}Na_{0.5}Nb_{0.92}Sb_{0.08}O_3$ + xmol%MnO_2 ceramics with $x = 0.5$, 1.0, 2.0 and 3.0 at 1 kHz as a function of temperature

at T_c in the plot of ε_r versus temperature as shown in Fig. 5a. However, the substitution of 8% Sb^{5+} for Nb^{5+} in the $K_{0.5}Na_{0.5}NbO_3$ + 0.5 mol%MnO_2 ceramic leads to a broadening of the transition peak at T_c, suggesting the appearance of a diffuse phase transition. A diffuse phase transition has been observed in many ABO_3-type perovskites and Bi-layered structure compounds, e.g. $Ba_{0.5}Na_{0.5}TiO_3$-based ceramics [17], $K_{0.5}La_{0.5}Bi_2Nb_2O_9$ [18], $Pb(Mg_{1/3}Nb_{2/3})O_3$ [19], KNN-$SrTiO_3$ [20]. The diffuseness in the phase transition can be determined from the modified Curie–Weiss law $1/\varepsilon_r - 1/\varepsilon_m = C^{-1}(T - T_m)^{\gamma}$ [19], where ε_m is the maximum value of relative permittivity at the phase transition temperature T_m, γ is the degree of diffuseness and C is the Curie-like constant. The γ can have a value ranging from 1 for a normal ferroelectric to 2 for an ideal relaxor ferroelectric.

Based on the temperature plots of ε_r at 10 kHz, the graphs of $\ln(1/\varepsilon_r - 1/\varepsilon_m)$ versus $\ln(T - T_m)$ for the $K_{0.5}Na_{0.5}NbO_3$ + 0.5 mol%MnO_2 and $K_{0.5}Na_{0.5}Nb_{0.92}Sb_{0.08}O_3$ + 0.5 mol%MnO_2 ceramics were plotted, giving the results shown in Fig. 6. Both the samples exhibit a linear relationship. By least-squared fitting the experimental data to the modified Curie–Weiss law, γ was determined. The calculated γ for the $K_{0.5}Na_{0.5}NbO_3$ + 0.5 mol%MnO_2 ceramic is 1.17, revealing the normal ferroelectric characteristic. After the substitution of 8 mol%Sb^{+}, γ increases significantly to 1.63, suggesting that the substitution of Sb^{5+} makes the $K_{0.5}Na_{0.5}Nb_{0.92}Sb_{0.08}O_3$ + 0.5 mol%MnO_2 ceramic become more relaxor, thus exhibiting a broadened transition peak as shown in Fig. 5b. The appearance of the diffuse phase transition may be ascribed to the increase in the disorder degree of B-site ions, resulting from the substitution of Sb^{5+} for Nb^{5+}.

Except for the $K_{0.5}Na_{0.5}Nb_{0.92}Sb_{0.08}O_3$ ceramic (i.e., without MnO_2 doping), all the ceramics can be well sintered at 1,080–1,110 °C and have a dense structure, giving a high relative density (>95%), and so exhibit a well-saturated *P-E* hysteresis loop under an electric field of 5 kV/mm. Figure 7a shows the *P-E* hysteresis loops of the $K_{0.5}Na_{0.5}Nb_{0.92}Sb_{0.08}O_3$ + xmol%MnO_2 ceramics with $x = 0.5$, 1.5 and 2.5, while the variations of the remanent polarization P_r and coercive field E_c with x are shown in Fig. 7b. For the $K_{0.5}Na_{0.5}Nb_{0.92}Sb_{0.08}O_3$ + xmol%MnO_2 ceramics, P_r increases slightly and then decreases as x increases from 0.5

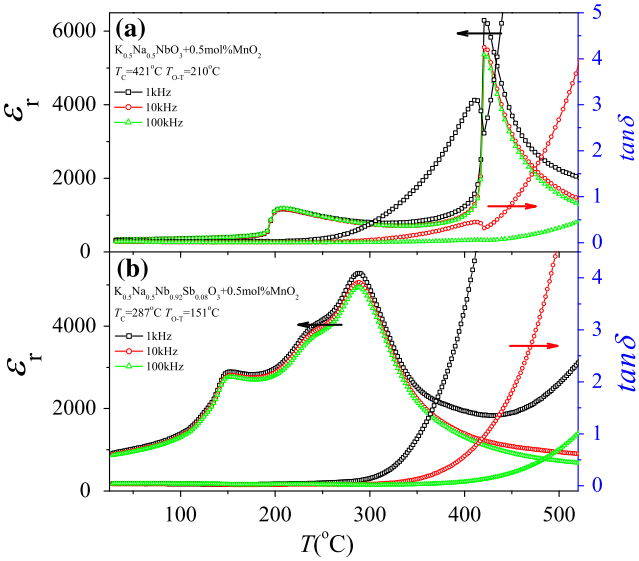

Fig. 5 Temperature dependences of relative permittivity ε_r and loss tangent tanδ of **a** $K_{0.5}Na_{0.5}NbO_3$ + 0.5 mol%MnO_2 ceramics and **b** $K_{0.5}Na_{0.5}Nb_{0.92}Sb_{0.08}O_3$ + xmol%MnO_2 ceramics

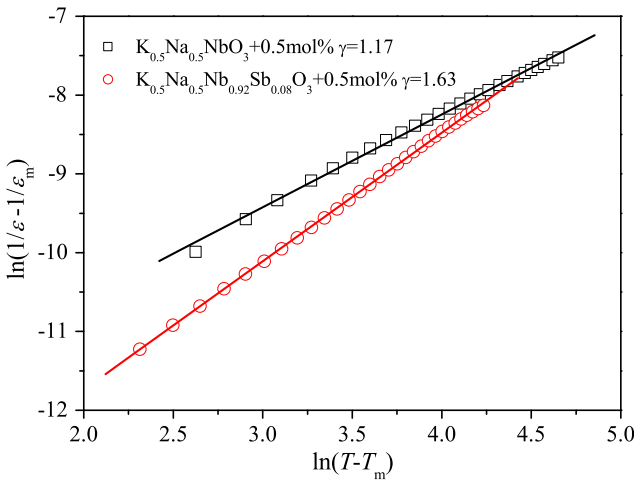

Fig. 6 Plot of $\ln(1/\varepsilon - 1/\varepsilon_m)$ versus $\ln(1/T - 1/T_m)$ for the $K_{0.5}Na_{0.5}NbO_3$ + 0.5 mol%MnO_2 ceramics and $K_{0.5}Na_{0.5}Nb_{0.92}Sb_{0.08}O_3$ + xmol%MnO_2 ceramics. The symbols denote experimental data while the solid lines denote the least-squared fitting line to the modified Curie–Weiss law

to 3.0, giving a maximum value of 26.8 μC/cm^2 at $x = 1.5$, while E_c increases considerably from 0.65 to 0.97 kV/mm with x increasing from 0.5 to 2.0 and then decreases slightly to 0.94 kV/mm with x further increasing to 3.0.

Figure 8 shows the variations of d_{33}, k_p, Q_m, ε_r and tanδ with x for the $K_{0.5}Na_{0.5}Nb_{0.92}Sb_{0.08}O_3$ + xmol%MnO_2 ceramics. After the use of the sintering aid, the density of the ceramics increases significantly from 4.12 to 4.48 (Fig. 3), thus yielding considerable enhancement in d_{33}, k_p, and Q_m and reduction in tanδ. The optimum content of MnO_2 is 0.5 mol%. It can be seen that because of the poor densification, the ceramic without MnO_2 doping exhibits the very high tanδ (65.2%) and relatively poor piezoelectricity ($d_{33} = 95$ pC/N, $k_p = 22.6\%$, $Q_m = 6$). After the addition of 0.5 mol%MnO_2, the tanδ decrease significantly and reaches a minimum value of 2.71%. The great decrease in tanδ should be ascribed to the great enhancement in densification. For the ceramic with $x = 0.5$, the good piezoelectric and dielectric properties are obtained: $d_{33} =$ 187 pC/N, $k_p = 47.2\%$, and $Q_m = 123$ (Fig. 8a), while $\varepsilon_r = 980$ and tan$\delta = 2.71\%$ (Fig. 8b).

Figure 9 shows the temperature dependence of k_p for the $K_{0.5}Na_{0.5}Nb_{0.92}Sb_{0.08}O_3$ + 0.5 mol%MnO_2 ceramic. It can be seen that for the $K_{0.5}Na_{0.5}Nb_{0.92}Sb_{0.08}O_3$ + 0.5 mol% MnO_2 ceramic, there has no depolarization below 120 °C. Because the $T_{O\text{-}T}$ is relatively high (151 °C), the $K_{0.5}Na_{0.5}Nb_{0.92}Sb_{0.08}O_3$ + 0.5 mol%MnO_2 ceramic exhibits a very good thermal characteristic. It can be seen that as temperature increases above $T_{O\text{-}T}$, the piezoelectricity of the ceramic become weak gradually.

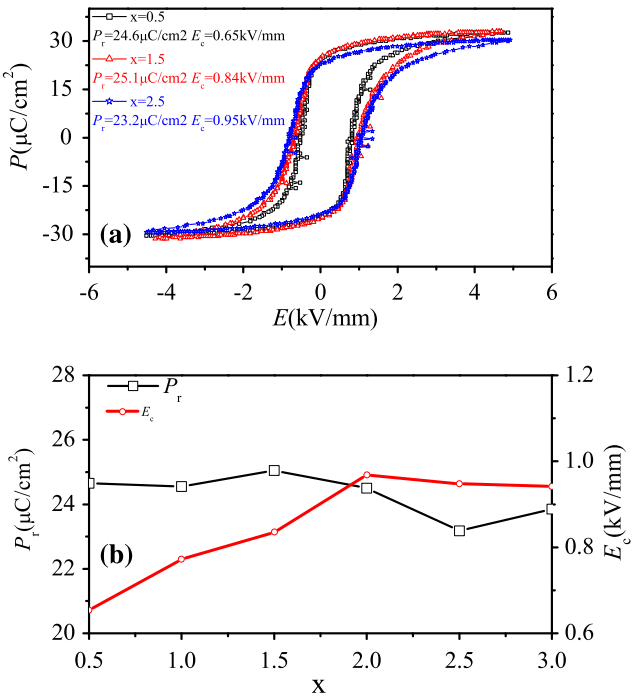

Fig. 7 **a** *P-E* hysteresis loops of the $K_{0.5}Na_{0.5}Nb_{0.92}Sb_{0.08}O_3$ + x-mol%MnO_2 ceramics with $x = 0.5$, 1.5 and 2.5; **b** Variations of P_r and E_c with x for the $K_{0.5}Na_{0.5}Nb_{0.92}Sb_{0.08}O_3$ + xmol%MnO_2 ceramics

Table 1 shows the electrical properties of $K_{0.5}Na_{0.5}Nb_{0.92}Sb_{0.08}O_3$ + 0.5 mol%MnO_2, $K_{0.5}Na_{0.5}NbO_3$ + 0.5 mol% MnO_2 and $K_{0.5}Na_{0.5}Nb_{0.92}Sb_{0.08}O_3$ (i.e., without MnO_2 doping) ceramics. It can be seen that compared with the $K_{0.5}Na_{0.5}Nb_{0.92}Sb_{0.08}O_3$ + 0.5 mol%MnO_2 ceramic, the $K_{0.5}Na_{0.5}NbO_3$ + 0.5 mol%MnO_2 ceramic exhibits typical "hardened" electrical characteristics (low d_{33}, k_p, ε_r, tanδ and P_r; high Q_m and E_c). After the substitution of 8% Sb^{5+} for Nb^{5+}, the observed d_{33}, k_p, ε_r, tanδ and P_r increase by about 68, 8, 200, 145 and 13%, respectively, while the observed Q_m and E_c decrease by about 63 and 13%, respectively. This suggests that after the substitution of 8% Sb^{5+} for Nb^{5+}, the ceramics become "softened", thus giving rise to significant improvements in d_{33}, k_p and ε_r. The improvement of piezoelectric properties of the ceramics should be attributed to the strong covalency of Sb. For the $K_{0.5}Na_{0.5}Nb_{0.92}Sb_{0.08}O_3$ + 0.5 mol%MnO_2 ceramic, the partial substitution of Sb^{5+} for Nb^{5+} induces a much stronger covalency in the KNN-based perovskite, which favors the ferroelectricity and piezoelectricity. It can be also noted that because of the poor densification, the MnO_2-undoped $K_{0.5}N_{a0.5}Nb_{0.92}Sb_{0.08}O_3$ ceramic possesses the very poor piezoelectricity, indicating the effectiveness of MnO_2 as a sintering aid for improving the sintering performance and electrical properties.

4 Conclusions

$K_{0.5}Na_{0.5}Nb_{0.92}Sb_{0.08}O_3$ + xmol%MnO_2 lead-free ceramics have been fabricated by an ordinary sintering technique. Our results show that MnO_2 is an excellent sintering aid for improving the sintering performance. A small amount of MnO_2 (0.5–1.0 mol%) improves effectively the densification. The high densification and strong covalence of Sb lead to the significant improvement in the ferroelectricity and piezoelectricity of the ceramics. The ceramic with $x = 0.5$ exhibits excellent ferroelectric and piezoelectric properties: $d_{33} = 187$ pC/N, $k_P = 47.2\%$, $\varepsilon_r = 980$, tan$\delta =$ 2.71%, $P_r = 24.7$ μC/cm^2, $E_c = 0.65$ kV/mm and $T_C =$ 287 °C. Because of high $T_{O\text{-}T}$, the ceramic with $x = 0.5$ exhibits a very good temperature stability of piezoelectric properties. Our results also show that the $K_{0.5}Na_{0.5}Nb_{0.92}Sb_{0.08}O_3$ + xmol%MnO_2 ceramics exhibit relaxor characteristic, which may be ascribed to the increase in the disorder degree of B-site ions resulting from the partial substitutions of Sb^{5+} for Nb^{5+}. It is suggested that the $K_{0.5}Na_{0.5}Nb_{0.92}Sb_{0.08}O_3$ + xmol%MnO_2 ($x = 0.5$–1.0) ceramics are an attractive candidate for lead-free ceramics.

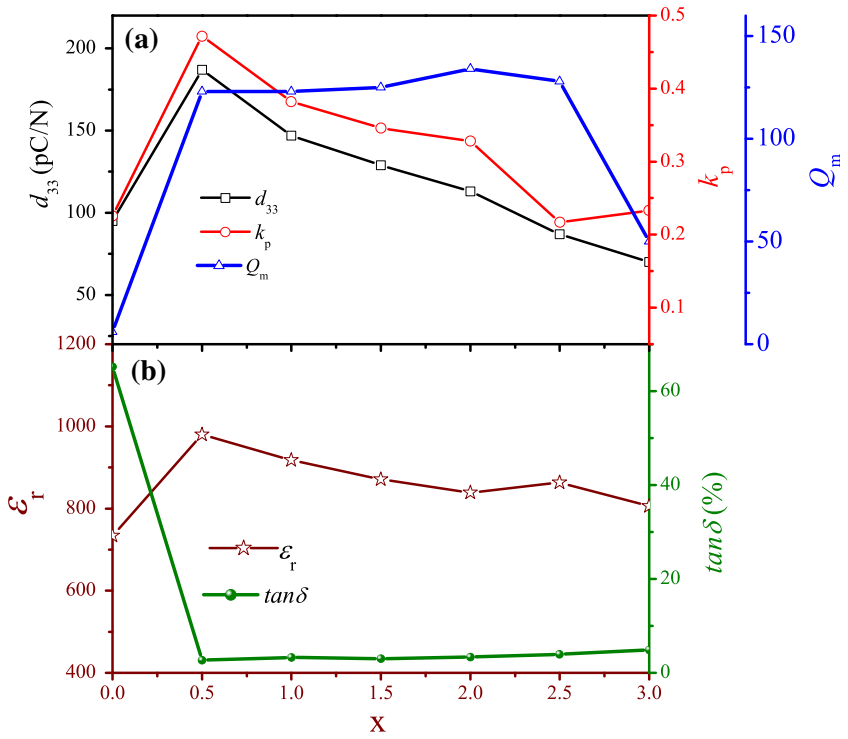

Fig. 8 Variations of d_{33}, k_p, Q_m, ε_r and tanδ with x for the $K_{0.5}Na_{0.5}Nb_{0.92}Sb_{0.08}O_3$ + xmol%MnO_2 ceramics

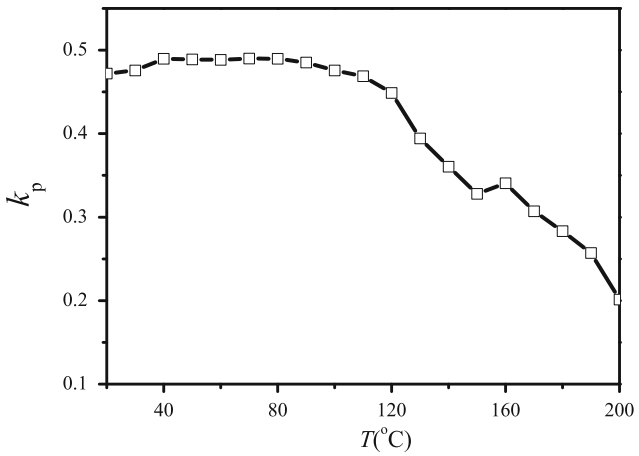

Fig. 9 Variation of k_p with temperature for the $K_{0.5}Na_{0.5}Nb_{0.92}Sb_{0.08}O_3$ + 0.5 mol%MnO_2 ceramic

Table 1 Electrical properties of (a) $K_{0.5}Na_{0.5}Nb_{0.92}Sb_{0.08}O_3$ + 0.5 mol%MnO_2, (b) $K_{0.5}Na_{0.5}NbO_3$ + 0.5 mol%MnO_2 and (c) $K_{0.5}Na_{0.5}Nb_{0.92}Sb_{0.08}O_3$ ceramics

	d_{33} (pC/N)	k_p (%)	Q_m	ε_r	tanδ (%)	P_r (μm/cm^2)	E_c (kV/mm)
a	187	47.2	123	980	2.71	24.7	0.65
b	111	43.8	330	322	1.10	21.8	0.75
c	95	22.6	6	734	65.2	–	–

Acknowledgment This work was supported by the project of Education Department of Sichuan Province (08ZA047), and Science and Technology Bureau of Sichuan Province (09ZQ026-059)

References

1. R.E. Jaeger, L. Egerton, J. Am. Ceram. Soc. **45**(5), 209 (1962)
2. L. Egerton, D.M. Dillom, J. Am. Ceram. Soc. **42**(9), 438 (1959)
3. Z.S. Ahn, W.A. Schulze, J. Am. Ceram. Soc. **70**(1), C18 (1987)
4. E. Hollenstein, M. Davis, D. Damjanovic, N. Setter. Appl. Phys. Lett. **87**, 182905 (2005)
5. G.Z. Zang, J.F. Wang, H.C. Chen, W.B. Su, C.M. Wang, P. Qi, B.Q. Ming, J. Du, L.M. Zheng, S. Zhang, R.T. Shrout, Appl. Phys. Lett. **88**, 212908 (2006)
6. D. Lin, K.W. Kwok, K.H. Lam, H.L.W. Chan, J. Appl. Phys. **101**, 074111 (2007)
7. H.Y. Park, C.W. Ahn, H.C. Song, J.H. Lee, S. Nahm, K. Uchino, H.G. Lee, H.J. Lee, Appl. Phys. Lett. **89**, 062906 (2006)
8. R. Zuo, C. Ye, Appl. Phys. Lett. **91**, 062916 (2007)
9. Y. Guo, K. Kakimoto, H. Ohsato, Appl. Phys. Lett. **85**, 4121 (2004)
10. R. Zuo, X. Fang, C. Ye, Appl. Phys. Lett. **90**, 092904 (2006)
11. Y. Saito, H. Takao, T. Tani, T. Nonoyama, K. Takatori, T. Homma, T. Nagaya, M. Nakamur, Nature **432**, 84 (2004)
12. M. Matsubara, K. Kikuta, S. Hirano, J. Appl. Phys. **97**, 114105 (2005)
13. H. Takao, Y. Saito, Y. Aoki, K. Horibuchi, J. Am. Ceram. Soc. **89**, 1951 (2006)
14. D.J. Singh, M. Ghita, S.V. Halilov, M. Fornari, J. Phys. IV **128**, 47 (2004)
15. C. Galassi, E. Roncari, C. Capiani, F. Craciun, J. Eur. Ceram. Soc. **19**(6–7), 1237 (1999)
16. C.S. Yu, H.L. Hsieh, J. Eur. Ceram. Soc. **25**(12), 2425 (2005)

17. Y. Li, W. Chen, Q. Xu, J. Zhou, X. Gu, S. Fang, Mater. Chem. Phys. **94**, 328 (2005)
18. C. Karthik, N. Ravishankar, K.B.R. Varma, Appl. Phys. Lett. **89**, 042905 (2006)
19. K. Uchino, S. Nomura, L.E. Cross, S.J. Tang, R.E. Newnham, J. Appl. Phys. **51**, 1142 (1980)
20. Y. Guo, K. Kakimoto, H. Ohsato, Solid State Commun. **129**, 279 (2004)